Aerosol particle formation in the upper residual layer

Authors:

Janne Lampilahti[1], Katri Leino[1], Antti Manninen[2], Pyry Poutanen[1], Anna Franck[1], Maija Peltola[1], Paula Hietala[1], Lisa Beck[1], Lubna Dada[1], Lauriane Quéléver[1], Ronja Öhrnberg[1], Ying Zhou[3], Madeleine Ekblom[1], Ville Vakkari[2,4], Sergej Zilitinkevich[1,2], Veli-Matti Kerminen[1], Tuukka Petäjä[1,5], Markku Kulmala[1,3,5]

Affiliations:

[1]Institute for Atmospheric and Earth System Research / Physics, Faculty of Science, University of Helsinki, Helsinki, Finland.
[2]Finnish Meteorological Institute, Helsinki, Finland.
[3]Aerosol and Haze Laboratory, Beijing Advanced Innovation Center for Soft Matter Science and Engineering, Beijing University of Chemical Technology, Beijing, China.
[4]Atmospheric Chemistry Research Group, Chemical Resource Beneficiation, North-West University, Potchefstroom, South Africa.
[5]Joint International Research Laboratory of Atmospheric and Earth System Sciences, Nanjing University, Nanjing, China.

Correspondence to: Janne Lampilahti (janne.lampilahti@helsinki.fi)

Abstract: According to current estimates, atmospheric new particle formation (NPF) produces a large fraction of aerosol particles and cloud condensation nuclei in the earth's atmosphere, therefore having implications for health and climate. Despite recent advances, atmospheric NPF is still insufficiently understood in the upper parts of the boundary layer (BL). In addition, it is unclear how NPF in upper BL is related to the processes observed in the near-surface layer. The role of the topmost part of the residual layer (RL) in NPF is to a large extent unexplored. This paper presents new results from co-located airborne and ground-based measurements in a boreal forest environment, showing that many NPF events (~42%) appear to start in the upper RL. The freshly formed particles may be entrained into the growing mixed layer (ML) where they continue to grow in size, similar to the aerosol particles formed within the ML. The results suggest that in the boreal forest environment, NPF in the upper RL has an important contribution to the aerosol load in the BL.

1. Introduction

It has been estimated that atmospheric new particle formation (NPF) is responsible for most of the cloud condensation nuclei (CCN) in the atmosphere (Dunne et al., 2016; Gordon et al., 2017; Pierce and Adams, 2009; Yu and Luo, 2009). Aerosol-cloud interactions, in turn, have important but poorly-understood effects on climate (Boucher et al., 2013). Being a major source of ultrafine

41   aerosol particles in many environments (e.g. Brines et al., 2015; Posner and Pandis, 2015; Salma et

42   al., 2017; Yu et al., 2019), NPF may have implications for human health.

43

44   The majority of NPF observations come from ground-based measurements (Kerminen et al., 2018;

45   Kulmala et al., 2004), which can be argued to represent NPF within the mixed layer (ML).

46   Measurements from aircrafts (e.g. Clarke and Kapustin, 2002; Rose et al., 2017) and high-altitude

47   research stations (e.g. Bianchi et al., 2016) demonstrate that NPF frequently takes place in the free

48   troposphere (FT). Entrainment of particles formed in the upper FT was identified as an important

49   source of CCN in the tropical boundary layer (BL) (Wang et al., 2016; Williamson et al., 2019).

50

51   To what extent NPF happens in the lower FT and in the upper parts of the BL is not clear. Freshly

52   formed particles were observed in the inversion capping a ML (Chen et al., 2018; Platis et al., 2015;

53   Siebert et al., 2004) and in turbulent layers inside the residual layer (RL) (Wehner et al., 2010). NPF

54   was frequently observed in the lower FT over a megacity in a year-long campaign (Quan et al.,

55   2017). Also Qi et al. (2019) reported NPF just above the ML over Yangtze River Delta. In the

56   marine BL, sub-10 nm particles were observed in the entrainment zone above a cloud topped BL

57   (Dadashazar et al., 2018). Layers of sub-10 nm particles, usually less than 500 m in thickness, were

58   often observed in the lower FT over a boreal forest environment (Leino et al., 2019; Schobesberger

59   et al., 2013; Väänänen et al., 2016). On the other hand, Junkermann and Hacker (2018) attributed

60   their observations of ultrafine particle layers to flue gas emissions from stacks with subsequent

61   chemistry taking place during air mass transport over long distances.

62

63   In this study we used co-located airborne and ground-based measurements to study NPF in the BL

64   over a boreal forest. We aimed to answer the following questions: (1) where, how often and why

65   does NPF take place in the upper parts of the BL, and (2) how the upper-BL NPF is related to

66   ground-based observations, and what implications this has for data interpretation.

67

68   **2. Materials and methods**

69

70   *2.1. Airborne measurements*

71

72   We used data from airborne measurement campaigns conducted between 2011 and 2018 around

73   Hyytiälä, Finland. Figure 1 shows the data availability from these measurements. Most of the flights

74   were carried out during spring and early autumn because that is when NPF events are most common

in Hyytiälä. Here we focused on the data that was measured within a 40-km radius from Hyytiälä.

The measurement setups changed slightly over the years. Detailed descriptions of the setups on

board can be found in our previous studies (Leino et al., 2019; Schobesberger et al., 2013;

Väänänen et al., 2016).

The instrumented aircraft was a Cessna 172 operated from the Tampere-Pirkkala airport (ICAO:

EFTP). The sample air was collected through an outside inlet into a main sampling line that was

inside the aircraft's cabin. The forward movement of the aircraft during flight provided adequate

flow rate inside the main sampling line. The flow rate was maintained at 47 lpm by using a manual

valve. The instruments drew air from the main sampling line using core sampling inlets. The

necessary flow rate to the instruments was provided by pumps. The flow rate in the main sampling

line corresponded to roughly isokinetic sampling at the core sampling inlets. The airspeed was kept

at 130 km/h during the measurement flights.

The on-board aerosol instruments considered in this study were an ultrafine condensation particle

counter (uCPC, TSI, model: 3776), measuring the >3 nm particle number concentration at a 1-s

time resolution, a particle size magnifier (PSM, Airmodus, model: A10) operated with a TSI 3010

CPC, measuring the >1.5 nm particle number concentration at a 1-s time resolution, and a custom-

built scanning mobility particle sizer (SMPS) with a short Hauke type DMA and a TSI 3010 CPC,

measuring the aerosol number size distribution in the size range of 10-400 nm at a 2-min time

resolution. In addition, basic meteorological data (temperature, relative humidity and pressure) and

water vapor concentration from Licor Li-840 gas analyzer were used.

Vertically, the measurement profiles extended approximately from 100 m to 3000 m above the

ground. This altitude range covered the ML, RL and roughly 1 km of the FT (Figure 2). The

measurement flights lasted about 2-3 hours and were flown mostly during the morning (~8:00-

12:00 local time) and the afternoon (~13:00-16:00 local time). Horizontally, the profiles were flown

perpendicular to mean wind in order to avoid the airplane's exhaust fumes.

2.2. Ground-based measurements

Comprehensive atmospheric measurements have been done at the SMEAR II station in Hyytiälä

(61°50'40" N, 24°17'13" E, 180 m above sea level) since 1996 (Hari and Kulmala, 2005).The

landscape around the site is flat and dominated by Scots pine forests, with small farms and lakes

scattered nearby. The station represents typical rural background conditions.

We used data from the BAECC (Biogenic Aerosols–Effects on Clouds and Climate) campaign,

which took place in Hyytiälä during Feb-Sep 2014 (Petäjä et al., 2016), to study the relationship

between BL evolution and NPF observed at the station. High spectral resolution lidar (HSRL)

measurements and meteorological balloon soundings released every 4 hours by the U.S. Department

of Energy ARM mobile facility allowed us to monitor the evolution of the BL (Nikandrova et al.,

2018).

From the HSRL data we looked at the values of backscatter cross section in order to see the

development of the ML during the day. The data were averaged into 30-m altitude bins and 10-min

temporal bins. The ground-based measurements during the BAECC campaign were also

supplemented by aircraft measurements using the instrumented Cessna. In case of missing

soundings, we also looked at the balloon soundings released from Jokioinen ~120 km south-west

from Hyytiälä (WMO: 02963).

The number size distribution of aerosol particles between 3 and 1000 nm was measured at the

station using a differential mobility particle sizer (DMPS, Aalto et al., 2001). A neutral cluster and

air ion spectrometer (NAIS, Airel Ltd., Mirme and Mirme, 2013) measured the number size

distribution of air ions and particles in the size ranges of 0.8-42 nm and 2-42 nm, respectively

(Manninen et al., 2009). The time resolutions of the DMPS and NAIS were 10 min and 4 min,

respectively. The vertical flux of particles >10 nm was measured by the eddy covariance method

from 23 m above ground, which is a couple of meters above the canopy (Buzorius et al., 2000).

Vertical profiles of horizontal and vertical winds were measured with a Halo Photonics Stream Line

scanning Doppler lidar since year 2016. The Halo Photonics Stream Line is a 1.5 µm pulsed

Doppler lidar with a heterodyne detector and 30-m range resolution, and the minimum range of the

instrument is 90 m (Pearson et al., 2009). At Hyytiälä, a vertical stare of 12 beams and integration

time of 40 s per beam is scheduled every 30 min, whereas the other scan types operated during the

30-min measurement cycle were not utilized in this study. The lidar data were corrected for a

background noise artifact (Vakkari et al., 2019). The turbulent kinetic energy (TKE) dissipation rate

was calculated from the vertical stare according to the method by O'Connor et al. (2010) with a

signal-to-noise-ratio threshold of 0.001 applied to the data. Data availability is limited by relatively

142 low aerosol concentration at Hyytiälä, but TKE dissipation rate can be retrieved on most days up to

143 the top of the BL.

144

145 **3. Results and discussion**

146

147 In the aircraft data we frequently observed a layer of nucleation mode (sub-25 nm) particles above

148 the ML. First we introduce how the phenomenon was observed in the airborne and ground-based

149 measurements using a case study. Then we show that the particle layers occurred in the topmost part

150 of the RL, by studying the average vertical profile of particle number-size distribution and

151 temperature as well as the BAECC data. Finally, by using the BAECC data, we associate the

152 nucleation mode particles in the upper RL to a specific signal in the ground-based measurements

153 and use the observations at the SMEAR II station to gather long-term statistics.

154

155 *3.1 Case study: May 2, 2017*

156

157 On May 2 during the measurement airplane's ascend over Hyytiälä, we observed a layer of freshly

158 formed aerosol particles approximately between 1200 and 2000 m above the ground, in the top parts

159 of the ML (Figure 3). The layer had increased number concentrations of sub-20 nm and sub-3 nm

160 particles. The small size of the particles suggests that they were recently formed in the atmosphere.

161 The lower edge of the aerosol particle layer was observed at 12:24 UTC. The airplane entered back

162 into the ML at 12:56 UTC and at this point there were no signs of the particle layer, but the particle

163 number concentration had increased inside the ML. On the same day, an early morning flight before

164 the sunrise was also performed. During this flight no elevated particle layer was observed below

165 3000 m, suggesting that this particle layer had been formed after the sunrise. The air masses came

166 from a non-polluted sector over the Arctic Ocean and northern Scandinavia.

167

168 After the aerosol layer was observed from the airplane during the ascend, a new particle mode with

169 a geometric mean diameter of about 10 nm suddenly appeared at the ground-level at 12:36 (Figure

170 4). The appearance of this new particle mode was characterized by a negative peak in the vertical

171 particle flux, suggesting that the particles had been mixed down from aloft.

172

173 We then studied the vertical profiles of meteorological quantities measured on board the Cessna on

174 May 2, and the turbulent kinetic energy (TKE) dissipation rate calculated from the Doppler lidar

175 measurements during May 1-2 (Figure 5). In the Doppler lidar measurements, the increase in the

TKE dissipation rate clearly reveals the development of the ML on both days. On May 1 the ML reached roughly 1700 m above the ground, while on May 2 the first potential temperature profile measured on board the Cessna revealed the presence of a stable layer (upper RL) at roughly the same altitude. This matches with the height of the aerosol particle layer in Figure 3. The Doppler lidar measurements further show that on May 2 the ML reached this height around the noon UTC, which is when the particle layer was observed to be mixing down. This leads us to hypothesize that NPF was taking place in the upper RL.

3.2 Evidence of NPF in the upper RL based on long-term measurements

We analyzed the airborne data measured during 2011-2018. We plotted the median and 75th percentile number size distributions measured on board the aircraft as a function of altitude during NPF event days (65 days out of 130 measurement days) between 09:00 and 12:00 (Figure 6). NPF event days are characterized by a new growing particle mode appearing in the sub-25 nm size range (Dal Maso et al., 2005). If aerosol formation in the upper RL occurs on less than half of the NPF event days, it might not be visible in the median plot, but might still appear in the 75th percentile plot.

Interestingly, in the 75th percentile plot a layer of nucleation mode particles is observed at 2500-3000 m above sea level. In the mean temperature profile, an inversion is observed at the same altitude level. The ML and RL are commonly capped by temperature inversions (Stull, 1988). In this case, the inversion is likely where on average the top of the RL was, since the the top of the ML was well below this altitude. The probable reason for the unusually deep RL is that the NPF event days tend to be sunny spring days and the ML can grow exceptionally high, which also leads to a very deep RL. The vertical profile of particle number size distribution supports the idea that NPF was taking place in the upper RL.

3.3 Connection between NPF in the upper RL and ground-based observations

With the BAECC dataset we wanted to investigate whether the sudden appearance of nucleation mode particles with downward particle flux was associated with the ML reaching the upper RL. This would not only test the hypothesis that NPF happens in the topmost part of the RL, but also provide us with a tool to identify upper RL NPF from the ground-based data alone.

We looked for cases where a new particle mode suddenly appeared in the nucleation mode size
range during the daytime and the appearance of the particles was associated with a downward
particle flux. We noted the times when the particles first appeared, and also estimated a confidence
interval of the observation. Then we checked if we could find out the height of the RL from balloon
soundings or the Cessna flights. We looked for an elevated temperature inversion that was roughly
at the same altitude as the ML of the previous day had reached. We noted the base height of the
temperature inversion and took this as the top of the RL. Then we followed the height of the new
ML from the HSRL measurements and noted the time when the ML reached the inversion base, also
estimating a confidence interval. Figure 7 illustrates an example for this procedure.

We found 8 cases during the campaign where the analysis could be fully carried out. Figure 8 shows
a strong positive correlation between the new particle mode appearance time and the time when the
ML reached the top of the RL. This suggests that the suddenly appearing nucleation mode particles
were entrained into the ML from the upper RL. We found only a weak positive correlation between
the new particle mode appearance time and the geometric mean diameter of particles in the new
mode at the moment they were first observed. This is probably explained by the NPF starting at
different times during the day and variability in growth rates, coupled with the small sample size.

3.4 Implications for classifying NPF events

Previous studies that classified NPF events observed in Hyytiälä have collected statistics on the
occurrence of suddenly appearing particle modes. For example Buenrostro Mazon et al., (2009)
collected statistics on "tail events" where a new particle mode appears at particle diameters greater
than 10 nm and grows for several hours. Dada et al., (2018) collected statistics on "transported
events" where elevated number concentration of 7-25 nm particles persisted for more than 1.5
hours, but no elevated number concentrations at smaller particle sizes were observed. It was found
that ~36% of the NPF events observed for over 10 years in Hyytiälä were transported events. They
occurred especially when the conditions inside the ML were less favorable for nucleation.

Here we found cases in the SMEAR II data between 2013 and 2017, in which a new growing
particle mode suddenly, without continuous growth from smallest detectable sizes (3 nm), appears
in the nucleation mode and is associated with a negative peak in the vertical particle flux. We also
noted cases where a new particle mode appears with a continuous growth from the smallest

243 detectable sizes. Based on the previous analysis we assume that in the former case NPF took place

244 in the upper RL and in the latter case inside the ML. The analysis included 1750 days.

245

246 The monthly fractions of the different cases are shown in Figure 9. We found that NPF within the

247 ML occurred on 13% of all the days and NPF in the upper RL on 7% of all the days. During spring

248 (Mar-May) the corresponding percentages were 31% and 17%. On many days NPF took place both

249 in the upper RL and within the ML. According to this analysis, NPF in the upper RL constitutes

250 42% of the NPF event days in Hyytiälä. Moreover, on 16% of the NPF event days NPF only took

251 place in the upper RL but not in the ML.

252

253 The gaseous precursors involved in NPF may end up in the upper RL because of mixing from the

254 surface during the previous day (e.g. organic vapors emitted from the forest or sulfuric acid,

255 ammonia and amines originating from human activities) or because of long-range transport in the

256 FT (e.g. iodine oxides from the ocean).

257

258 Many factors favor NPF at higher altitudes, including enhanced photochemistry, reduced sinks and

259 reduced temperature. However, the unique NPF inducing features of the upper RL are probably

260 linked to the mixing that takes place in the interface between RL and FT. For example Nilsson and

261 Kulmala, (1998) found that mixing two air parcels with different initial temperatures and precursor

262 vapor concentrations can lead to a considerable increase in the nucleation rate.

263

264 If the new ML reaches the upper RL, particles formed originally in the RL will be mixed into the

265 ML where they continue to grow in size as low-volatility vapors present in the ML are able to

266 condense onto these particles. The processes are illustrated in Figure 10. In case the particles will

267 not be mixed down, they may persist in the FT for a longer time period and possibly have stronger

268 contribution to cloud formation.

269

270 ***4. Conclusions***

271

272 We measured aerosol particles, trace gases and meteorological parameters on board an instrumented

273 Cessna 172 over a boreal forest in Hyytiälä, Finland. The airborne data was complemented by the

274 continuous, comprehensive ground-based measurements at the SMEAR II station.

275

276 We found multiple evidence that NPF frequently takes place in the topmost part of the RL. This is

277 likely related to the unique thermodynamic conditions present in this layer due to mixing between

278 RL and FT air. We estimate that NPF in the upper RL occurs on 42% of the NPF event days in

279 Hyytiälä. Our results provide new information on NPF in the BL and they should be taken into

280 account when interpreting and analyzing ground-based as well as airborne measurements of aerosol

281 particles.

282

283 **Data availability:** The particle flux and DMPS data can be accessed from https://avaa.tdata.fi/web/

284 smart/smear (Junninen et al., 2009; last access: Oct 1, 2020). The BAECC HSRL and radiosonde

285 data is available from https://adc.arm.gov/discovery/ (Bambha et al., 2014; Keeler et al., 2014); last

286 access: Oct 1, 2020). The Jokioinen soundings can be accessed using the Finnish Meteorological

287 Institute's open data service https://en.ilmatieteenlaitos.fi/open-data (last access: Oct 1, 2020). The

288 ERA5 dataset can be accessed from https://cds.climate.copernicus.eu/cdsapp#!/home (last access:

289 May 6, 2020). The rest of the data was gathered into a dataset that can be accessed from

290 https://zenodo.org/record/4063662#.X3cHQnUzY88 (Lampilahti et al., 2020; last access: Oct 2,

291 2020).

292

293 **Author contribution:** JL, KL, AM, PP, AF, MP, PH, LD and LJQ conducted the airborne

294 measurements in 2017. PP wrote processing script for the airborne data. RÖ classified the SMEAR

295 II data for NPF events between 2013-2017. LB contributed to the data analysis. YZ and ME

296 analyzed the airborne data between 2011-2018. VV provided the Doppler lidar data. JL prepared the

297 manuscript with contributions from all co-authors.

298

299 **Acknowledgements:** This project has received funding from the ERC advanced grant No. 742206,

300 the European Union's Horizon 2020 research and innovation program under grant agreement No.

301 654109, the Academy of Finland Center of Excellence project No. 272041. SZ acknowledges

302 support from the Academy of Finland grant 314 798/799. We thank Erkki Järvinen and the pilots at

303 Airspark Oy for operating the research airplane and we are grateful for their hospitality and

304 helpfulness.

305

306 **References**

307

Aalto, P., Hämeri, K., Becker, E., Weber, R., Salm, J., Mäkelä, J. M., Hoell, C., O'Dowd, C. D., Hansson, H.-C., Väkevä, M., Koponen, I. K., Buzorius, G. and Kulmala, M.: Physical characterization of aerosol particles during nucleation events, Tellus B, 53(4), 344–358, doi:10.3402/tellusb.v53i4.17127, 2001.

Bambha, R., Eloranta, E., Garcia, J., Ermold, B. and Goldsmith, J.: High Spectral Resolution Lidar (HSRL), Atmospheric Radiat. Meas. ARM User Facil., doi:10.5439/1025200, 2014.

Bianchi, F., Tröstl, J., Junninen, H., Frege, C., Henne, S., Hoyle, C. R., Molteni, U., Herrmann, E., Adamov, A., Bukowiecki, N., Chen, X., Duplissy, J., Gysel, M., Hutterli, M., Kangasluoma, J., Kontkanen, J., Kürten, A., Manninen, H. E., Münch, S., Peräkylä, O., Petäjä, T., Rondo, L., Williamson, C., Weingartner, E., Curtius, J., Worsnop, D. R., Kulmala, M., Dommen, J. and Baltensperger, U.: New particle formation in the free troposphere: A question of chemistry and timing, Science, aad5456, doi:10.1126/science.aad5456, 2016.

Boucher, O., Randall, D., Artaxo, P., Bretherton, C., Feingold, G., Forster, P., Kerminen, V.-M., Kondo, Y., Liao, H., Lohmann, U., Rasch, P., Satheesh, S. K., Sherwood, S., Stevens, B. and Zhang, X. Y.: Clouds and Aerosols, in Climate Change 2013: The Physical Science Basis. Contribution of Working Group I to the Fifth Assessment Report of the Intergovernmental Panel on Climate Change, edited by T. F. Stocker, D. Qin, G.-K. Plattner, M. Tignor, S. K. Allen, J. Boschung, A. Nauels, Y. Xia, V. Bex, and P. M. Midgley, pp. 571–658, Cambridge University Press, Cambridge, United Kingdom and New York, NY, USA. [online] Available from: www.climatechange2013.org, 2013.

Brines, M., Dall'Osto, M., Beddows, D. C. S., Harrison, R. M., Gómez-Moreno, F., Núñez, L., Artíñano, B., Costabile, F., Gobbi, G. P., Salimi, F., Morawska, L., Sioutas, C. and Querol, X.: Traffic and nucleation events as main sources of ultrafine particles in high-insolation developed world cities, Atmospheric Chem. Phys., 15(10), 5929–5945, doi:https://doi.org/10.5194/acp-15-5929-2015, 2015.

Buenrostro Mazon, S., Riipinen, I., Schultz, D. M., Valtanen, M., Maso, M. D., Sogacheva, L., Junninen, H., Nieminen, T., Kerminen, V.-M. and Kulmala, M.: Classifying previously undefined days from eleven years of aerosol-particle-size distribution data from the SMEAR II station, Hyytiälä, Finland, Atmospheric Chem. Phys., 9(2), 667–676, doi:https://doi.org/10.5194/acp-9-667-2009, 2009.

Buzorius, G., Rannik, Ü., Mäkelä, J. M., Keronen, P., Vesala, T. and Kulmala, M.: Vertical aerosol fluxes measured by the eddy covariance method and deposition of nucleation mode particles above a Scots pine forest in southern Finland, J. Geophys. Res. Atmospheres, 105(D15), 19905–19916, doi:10.1029/2000JD900108, 2000.

Chen, H., Hodshire, A. L., Ortega, J., Greenberg, J., McMurry, P. H., Carlton, A. G., Pierce, J. R., Hanson, D. R. and Smith, J. N.: Vertically resolved concentration and liquid water content of atmospheric nanoparticles at the US DOE Southern Great Plains site, Atmospheric Chem. Phys., 18(1), 311–326, doi:https://doi.org/10.5194/acp-18-311-2018, 2018.

Clarke, A. D. and Kapustin, V. N.: A Pacific Aerosol Survey. Part I: A Decade of Data on Particle Production, Transport, Evolution, and Mixing in the Troposphere, J. Atmospheric Sci., 59(3), 363–382, doi:10.1175/1520-0469(2002)059<0363:APASPI>2.0.CO;2, 2002.

Dada, L., Chellapermal, R., Buenrostro Mazon, S., Paasonen, P., Lampilahti, J., Manninen, H. E., Junninen, H., Petäjä, T., Kerminen, V.-M. and Kulmala, M.: Refined classification and characterization of atmospheric new-particle formation events using air ions, Atmospheric Chem. Phys., 18(24), 17883–17893, doi:https://doi.org/10.5194/acp-18-17883-2018, 2018.

Dadashazar, H., Braun, R. A., Crosbie, E., Chuang, P. Y., Woods, R. K., Jonsson, H. H. and Sorooshian, A.: Aerosol characteristics in the entrainment interface layer in relation to the marine boundary layer and free troposphere, Atmospheric Chem. Phys., 18(3), 1495–1506, doi:https://doi.org/10.5194/acp-18-1495-2018, 2018.

Dal Maso, M., Kulmala, M., Riipinen, I., Wagner, R., Hussein, T., Aalto, P. P. and Lehtinen, K. E.: Formation and growth of fresh atmospheric aerosols: eight years of aerosol size distribution data from SMEAR II, Hyytiälä, Finland, Boreal Environ. Res., 10(5), 323, 2005.

Dunne, E. M., Gordon, H., Kürten, A., Almeida, J., Duplissy, J., Williamson, C., Ortega, I. K., Pringle, K. J., Adamov, A., Baltensperger, U., Barmet, P., Benduhn, F., Bianchi, F., Breitenlechner, M., Clarke, A., Curtius, J., Dommen, J., Donahue, N. M., Ehrhart, S., Flagan, R. C., Franchin, A., Guida, R., Hakala, J., Hansel, A., Heinritzi, M., Jokinen, T., Kangasluoma, J., Kirkby, J., Kulmala, M., Kupc, A., Lawler, M. J., Lehtipalo, K., Makhmutov, V., Mann, G., Mathot, S., Merikanto, J., Miettinen, P., Nenes, A., Onnela, A., Rap, A., Reddington, C. L. S., Riccobono, F., Richards, N. A. D., Rissanen, M. P., Rondo, L., Sarnela, N., Schobesberger, S., Sengupta, K., Simon, M., Sipilä, M., Smith, J. N., Stozhkov, Y., Tomé, A., Tröstl, J., Wagner, P. E., Wimmer, D., Winkler, P. M., Worsnop, D. R. and Carslaw, K. S.: Global atmospheric particle formation from CERN CLOUD measurements, Science, 354(6316), 1119–1124, doi:10.1126/science.aaf2649, 2016.

Gordon, H., Kirkby, J., Baltensperger, U., Bianchi, F., Breitenlechner, M., Curtius, J., Dias, A., Dommen, J., Donahue, N. M., Dunne, E. M., Duplissy, J., Ehrhart, S., Flagan, R. C., Frege, C., Fuchs, C., Hansel, A., Hoyle, C. R., Kulmala, M., Kürten, A., Lehtipalo, K., Makhmutov, V., Molteni, U., Rissanen, M. P., Stozhkov, Y., Tröstl, J., Tsagkogeorgas, G., Wagner, R., Williamson, C., Wimmer, D., Winkler, P. M., Yan, C. and Carslaw, K. S.: Causes and importance of new particle formation in the present-day and preindustrial atmospheres, J. Geophys. Res. Atmospheres, 122(16), 8739–8760, doi:10.1002/2017JD026844, 2017.

Hari, P. and Kulmala, M.: Station for measuring ecosystem-atmosphere relations (SMEAR II), Boreal Environ. Res., 10(5), 315–322, 2005.

Junninen, H., Lauri, A., Keronen, P., Aalto, P., Hiltunen, V., Hari, P. and Kulmala, M.: Smart-SMEAR: on-line data exploration and visualization tool tor SMEAR stations., Boreal Environ. Res., 14(4), 447–457, 2009.

Keeler, E., Coulter, R., Kyrouac, J. and Holdridge, D.: Balloon-Borne Sounding System (SONDEWNPN), Atmospheric Radiat. Meas. ARM User Facil., doi:10.5439/1021460, 2014.

Kerminen, V.-M., Chen, X., Vakkari, V., Petäjä, T., Kulmala, M. and Bianchi, F.: Atmospheric new particle formation and growth: review of field observations, Environ. Res. Lett., 13(10), 103003, doi:10.1088/1748-9326/aadf3c, 2018.

Kulmala, M., Vehkamäki, H., Petäjä, T., Dal Maso, M., Lauri, A., Kerminen, V.-M., Birmili, W. and McMurry, P. H.: Formation and growth rates of ultrafine atmospheric particles: a review of observations, J. Aerosol Sci., 35(2), 143–176, doi:10.1016/j.jaerosci.2003.10.003, 2004.

Lampilahti, J., Leino, K., Manninen, A., Poutanen, P., Franck, A., Peltola, M., Hietala, P., Beck, L., Dada, L., Quéléver, L., Öhrnberg, R., Zhou, Y., Ekblom, M., Vakkari, V., Zilitinkevich, S., Kerminen, V.-M., Petäjä, T. and Kulmala, M.: Aerosol particle formation in the upper residual layer: dataset, Zenodo, doi:10.5281/zenodo.4063662, 2020.

Leino, K., Lampilahti, J., Poutanen, P., Väänänen, R., Manninen, A., Buenrostro Mazon, S., Dada, L., Franck, A., Wimmer, D., Aalto, P. P., Ahonen, L. R., Enroth, J., Kangasluoma, J., Keronen, P., Korhonen, F., Laakso, H., Matilainen, T., Siivola, E., Manninen, H. E., Lehtipalo, K., Kerminen, V.-M., Petäjä, T. and Kulmala, M.: Vertical profiles of sub-3 nm particles over the boreal forest, Atmospheric Chem. Phys., 19(6), 4127–4138, doi:10.5194/acp-19-4127-2019, 2019.

Manninen, H. E., Petäjä, T., Asmi, E., Riipinen, N., Nieminen, T., Mikkilä, J., Horrak, U., Mirme, A., Mirme, S., Laakso, L., Kerminen, V.-M. and Kulmala, M.: Long-term field measurements of charged and neutral clusters using Neutral cluster and Air Ion Spectrometer (NAIS), Boreal Environ. Res., 14(4), 591–605, 2009.

Mirme, S. and Mirme, A.: The mathematical principles and design of the NAIS – a spectrometer for the measurement of cluster ion and nanometer aerosol size distributions, Atmospheric Meas. Tech., 6(4), 1061–1071, doi:10.5194/amt-6-1061-2013, 2013.

Nikandrova, A., Tabakova, K., Manninen, A., Väänänen, R., Petäjä, T., Kulmala, M., Kerminen, V.-M. and O'Connor, E.: Combining airborne in situ and ground-based lidar measurements for attribution of aerosol layers, Atmospheric Chem. Phys., 18(14), 10575–10591, doi:https://doi.org/10.5194/acp-18-10575-2018, 2018.

Nilsson, E. D. and Kulmala, M.: The potential for atmospheric mixing processes to enhance the binary nucleation rate, J. Geophys. Res. Atmospheres, 103(D1), 1381–1389, doi:10.1029/97JD02629, 1998.

O'Connor, E. J., Illingworth, A. J., Brooks, I. M., Westbrook, C. D., Hogan, R. J., Davies, F. and Brooks, B. J.: A Method for Estimating the Turbulent Kinetic Energy Dissipation Rate from a Vertically Pointing Doppler Lidar, and Independent Evaluation from Balloon-Borne In Situ Measurements, J. Atmospheric Ocean. Technol., 27(10), 1652–1664, doi:10.1175/2010JTECHA1455.1, 2010.

Pearson, G., Davies, F. and Collier, C.: An Analysis of the Performance of the UFAM Pulsed Doppler Lidar for Observing the Boundary Layer, J. Atmospheric Ocean. Technol., 26(2), 240–250, doi:10.1175/2008JTECHA1128.1, 2009.

Petäjä, T., O'Connor, E. J., Moisseev, D., Sinclair, V. A., Manninen, A. J., Väänänen, R., von Lerber, A., Thornton, J. A., Nicoll, K., Petersen, W., Chandrasekar, V., Smith, J. N., Winkler, P. M., Krüger, O., Hakola, H., Timonen, H., Brus, D., Laurila, T., Asmi, E., Riekkola, M.-L., Mona, L., Massoli, P., Engelmann, R., Komppula, M., Wang, J., Kuang, C., Bäck, J., Virtanen, A., Levula, J., Ritsche, M. and Hickmon, N.: BAECC: A Field Campaign to Elucidate the Impact of Biogenic Aerosols on Clouds and Climate, Bull. Am. Meteorol. Soc., 97(10), 1909–1928, doi:10.1175/BAMS-D-14-00199.1, 2016.

Pierce, J. R. and Adams, P. J.: Uncertainty in global CCN concentrations from uncertain aerosol nucleation and primary emission rates, Atmospheric Chem. Phys., 9(4), 1339–1356, doi:10.5194/acp-9-1339-2009, 2009.

Platis, A., Altstädter, B., Wehner, B., Wildmann, N., Lampert, A., Hermann, M., Birmili, W. and Bange, J.: An Observational Case Study on the Influence of Atmospheric Boundary-Layer Dynamics on New Particle Formation, Bound.-Layer Meteorol., 158(1), 67–92, doi:10.1007/s10546-015-0084-y, 2015.

Posner, L. N. and Pandis, S. N.: Sources of ultrafine particles in the Eastern United States, Atmos. Environ., 111, 103–112, doi:10.1016/j.atmosenv.2015.03.033, 2015.

Qi, X., Ding, A., Nie, W., Chi, X., Huang, X., Xu, Z., Wang, T., Wang, Z., Wang, J., Sun, P., Zhang, Q., Huo, J., Wang, D., Bian, Q., Zhou, L., Zhang, Q., Ning, Z., Fei, D., Xiu, G. and Fu, Q.: Direct measurement of new particle formation based on tethered airship around the top of the planetary boundary layer in eastern China, Atmos. Environ., 209, 92–101, doi:10.1016/j.atmosenv.2019.04.024, 2019.

Quan, J., Liu, Y., Liu, Q., Jia, X., Li, X., Gao, Y., Ding, D., Li, J. and Wang, Z.: Anthropogenic pollution elevates the peak height of new particle formation from planetary boundary layer to lower free troposphere, Geophys. Res. Lett., 44(14), 7537–7543, doi:10.1002/2017GL074553, 2017.

Rose, C., Sellegri, K., Moreno, I., Velarde, F., Ramonet, M., Weinhold, K., Krejci, R., Andrade, M., Wiedensohler, A., Ginot, P. and Laj, P.: CCN production by new particle formation in the free troposphere, Atmospheric Chem. Phys., 17(2), 1529–1541, doi:https://doi.org/10.5194/acp-17-1529-2017, 2017.

Salma, I., Varga, V. and Németh, Z.: Quantification of an atmospheric nucleation and growth process as a single source of aerosol particles in a city, Atmospheric Chem. Phys., 17(24), 15007–15017, doi:https://doi.org/10.5194/acp-17-15007-2017, 2017.

Schobesberger, S., Väänänen, R., Leino, K., Virkkula, A., Backman, J., Pohja, T., Siivola, E., Franchin, A., Mikkilä, J., Paramonov, M., Aalto, P. P., Krejci, R., Petäjä, T. and Kulmala, M.: Airborne measurements over the boreal forest of southern Finland during new particle formation events in 2009 and 2010, Boreal Environ. Res., 18(2), 145–164, 2013.

Siebert, H., Stratmann, F. and Wehner, B.: First observations of increased ultrafine particle number concentrations near the inversion of a continental planetary boundary layer and its relation to ground-based measurements, Geophys. Res. Lett., 31(9), doi:10.1029/2003GL019086, 2004.

Stull, R. B.: An Introduction to Boundary Layer Meteorology, Softcover reprint of the original 1st ed. 1988 edition., Springer, Dordrecht., 1988.

Väänänen, R., Krejci, R., Manninen, H. E., Manninen, A., Lampilahti, J., Buenrostro Mazon, S., Nieminen, T., Yli-Juuti, T., Kontkanen, J., Asmi, A., Aalto, P. P., Keronen, P., Pohja, T., O'Connor, E., Kerminen, V.-M., Petäjä, T. and Kulmala, M.: Vertical and horizontal variation of aerosol number size distribution in the boreal environment, Atmospheric Chem. Phys. Discuss., Manuscript in review, doi:10.5194/acp-2016-556, 2016.

Vakkari, V., Manninen, A. J., O'Connor, E. J., Schween, J. H., Zyl, P. G. van and Marinou, E.: A novel post-processing algorithm for Halo Doppler lidars, Atmospheric Meas. Tech., 12(2), 839–852, doi:https://doi.org/10.5194/amt-12-839-2019, 2019.

Wang, J., Krejci, R., Giangrande, S., Kuang, C., Barbosa, H. M. J., Brito, J., Carbone, S., Chi, X., Comstock, J., Ditas, F., Lavric, J., Manninen, H. E., Mei, F., Moran-Zuloaga, D., Pöhlker, C., Pöhlker, M. L., Saturno, J., Schmid, B., Souza, R. A. F., Springston, S. R., Tomlinson, J. M., Toto, T., Walter, D., Wimmer, D., Smith, J. N., Kulmala, M., Machado, L. A. T., Artaxo, P., Andreae, M. O., Petäjä, T. and Martin, S. T.: Amazon boundary layer aerosol concentration sustained by vertical transport during rainfall, Nature, 539(7629), 416–419, doi:10.1038/nature19819, 2016.

Wehner, B., Siebert, H., Ansmann, A., Ditas, F., Seifert, P., Stratmann, F., Wiedensohler, A., Apituley, A., Shaw, R. A., Manninen, H. E. and Kulmala, M.: Observations of turbulence-induced new particle formation in the residual layer, Atmospheric Chem. Phys., 10(9), 4319–4330, doi:10.5194/acp-10-4319-2010, 2010.

Williamson, C. J., Kupc, A., Axisa, D., Bilsback, K. R., Bui, T., Campuzano-Jost, P., Dollner, M., Froyd, K. D., Hodshire, A. L., Jimenez, J. L., Kodros, J. K., Luo, G., Murphy, D. M., Nault, B. A., Ray, E. A., Weinzierl, B., Wilson, J. C., Yu, F., Yu, P., Pierce, J. R. and Brock, C. A.: A large source of cloud condensation nuclei from new particle formation in the tropics, Nature, 574(7778), 399–403, doi:10.1038/s41586-019-1638-9, 2019.

Yu, F. and Luo, G.: Simulation of particle size distribution with a global aerosol model: contribution of nucleation to aerosol and CCN number concentrations, Atmospheric Chem. Phys., 9(20), 7691–7710, 2009.

Yu, X., Venecek, M., Kumar, A., Hu, J., Tanrikulu, S., Soon, S.-T., Tran, C., Fairley, D. and Kleeman, M. J.: Regional sources of airborne ultrafine particle number and mass concentrations in California, Atmospheric Chem. Phys., 19(23), 14677–14702, doi:https://doi.org/10.5194/acp-19-14677-2019, 2019.
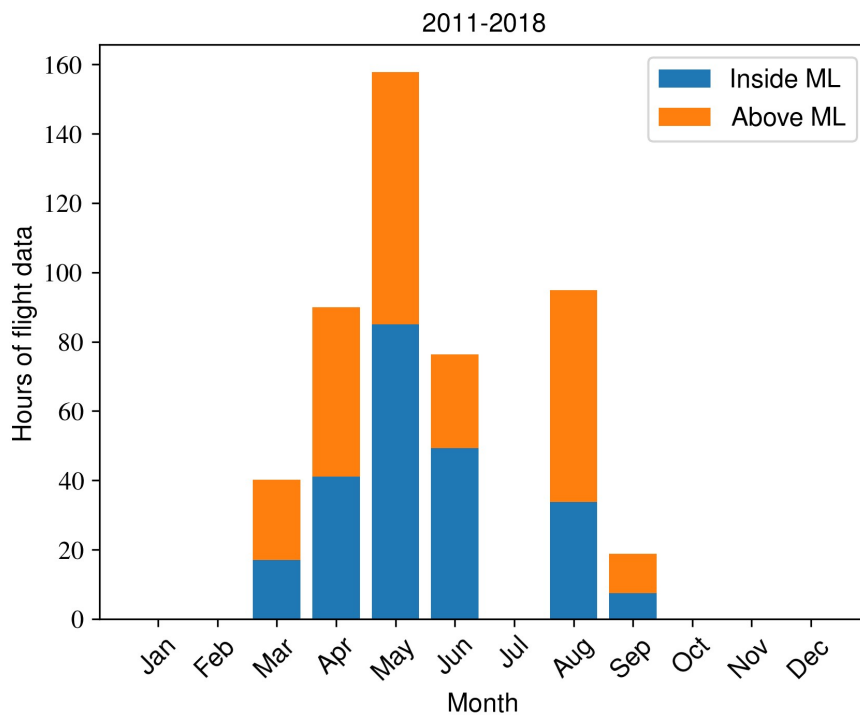
Figure 1: Monthly airborne data availability between 2011-2018 divided into measurements above and below the ML, based on the ML height obtained from the ERA5 reanalysis data.
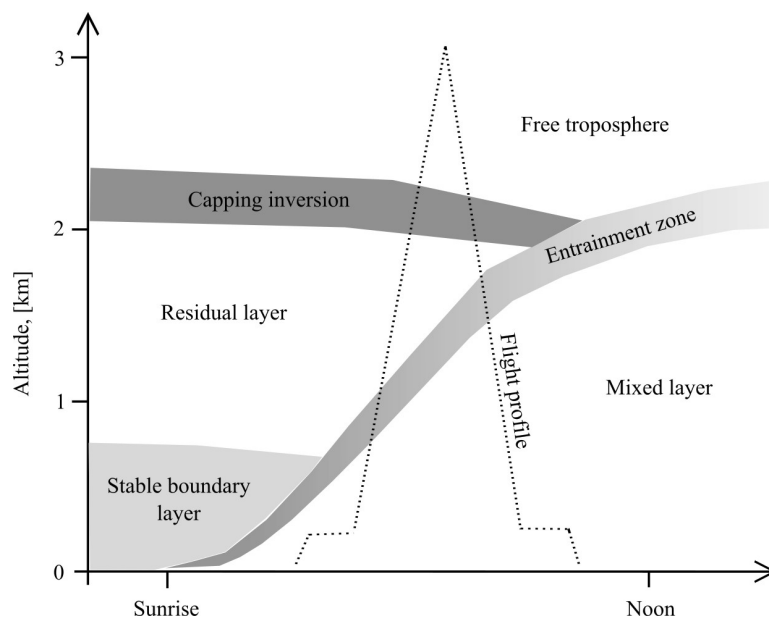
Figure 2: A schematic diagram of an average flight profile in relation to boundary layer evolution.

308
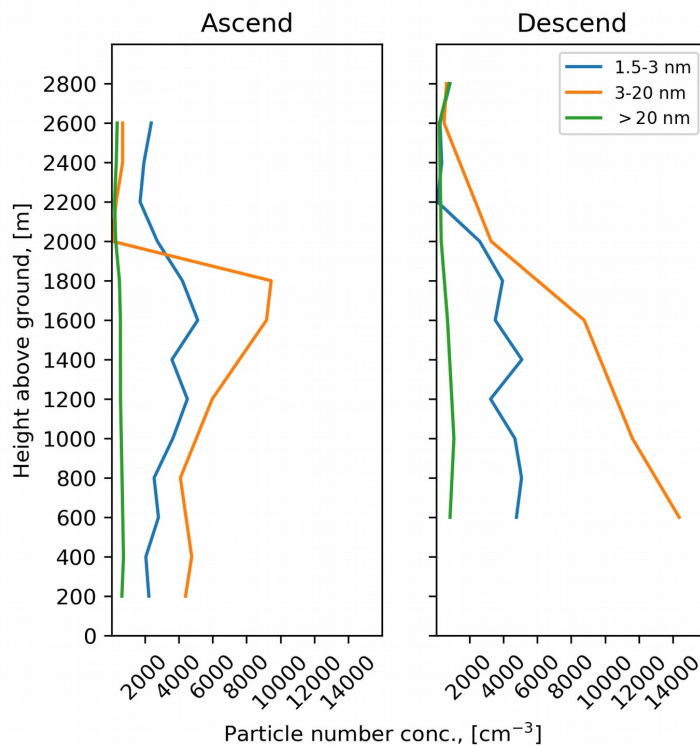
Figure 3: Vertical profiles of aerosol particle number concentration in three different size ranges (1.5-3 nm, 3-20 nm and >20 nm). The measurement profile was done on May 2, 2017 between 09:30 and 12:00 UTC.
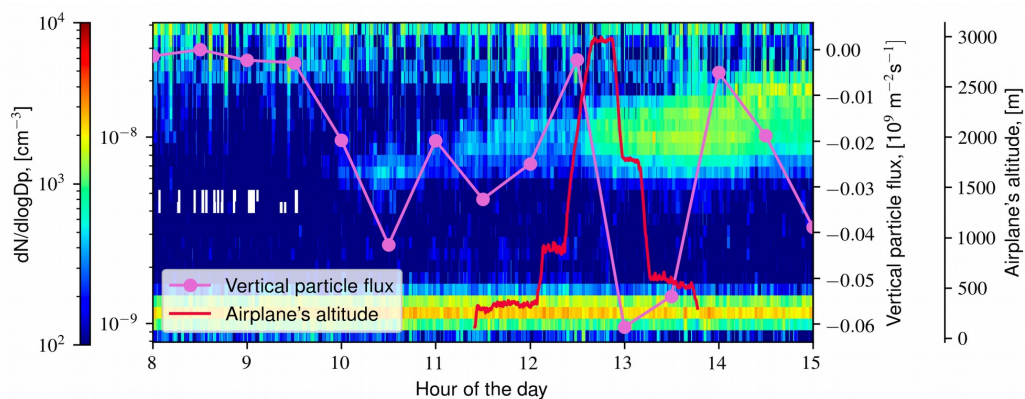
Figure 4: Positive ion number-size distribution measured at the SMEAR II station on May 2, 2017. The vertical flux of >10 nm particles and the airplane's altitude profile are superimposed. Negative means downward and positive upward particle flux.
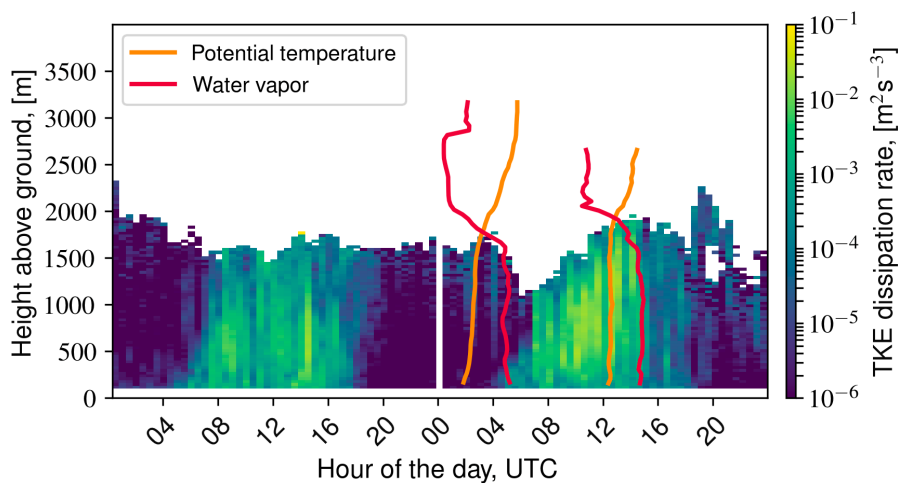
Figure 5: Turbulent kinetic energy (TKE) dissipation rate measured by the Doppler lidar in Hyytiälä between May 1-2, 2017. In addition the vertical profiles of potential temperature and water vapor concentration are shown from both the night and the afternoon Cessna flights on May 2, 2017.
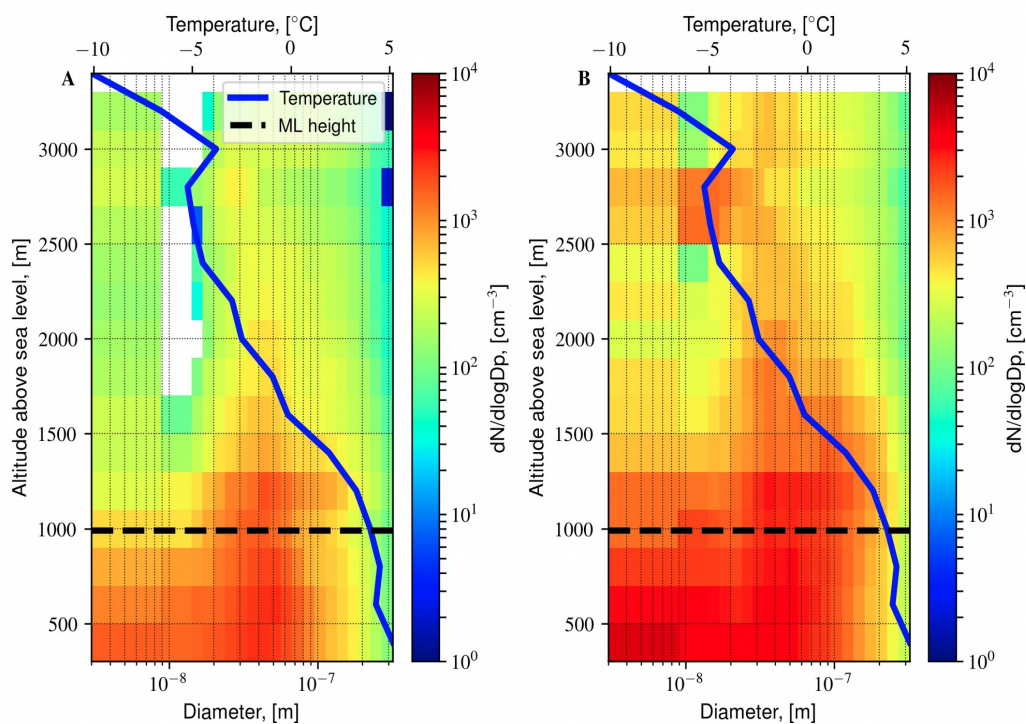
Figure 6: Panel A shows the median and panel B the 75th percentile vertical profile of particle number-size distribution measured on board the Cessna on NPF event days between 9-12 AM. The number-size distribution was binned into 200 m altitude bins. The data is from the campaigns conducted between 2011 and 2018. It includes only the data that was measured within 40 km radius from Hyytiälä. The dashed line is the mean ML height obtained from the ERA5 reanalysis data. The blue line is the mean temperature profile measured on board the airplane.
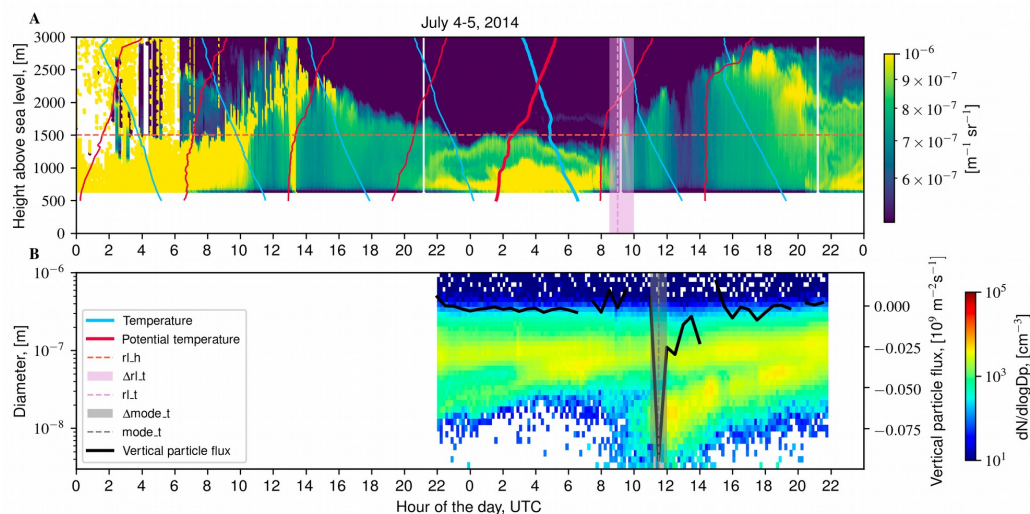
Figure 7: Panel A shows the backscatter cross section measured by the HSRL. The development of the ML is visible from the backscatter cross section signal. Temperature and potential temperature profiles from the 4-hourly balloon soundings are superimposed. The horizontal line rl_h refers to the height of the inversion base observed during the early morning of July 5th. The bold temperature and potential temperature profiles mark the sounding from which rl_h was determined. The rl_t and Δrl_t refer to the time when the ML was estimated to reach the rl_h and the confidence interval for this time respectively. Panel B shows the particle number-size distribution measured at the SMEAR II station, the black line is the vertical particle flux. The mode_t and Δmode_t respectively refer to the time and the confidence interval, when a nucleation particle mode that is associated with downward particle flux suddenly appears.
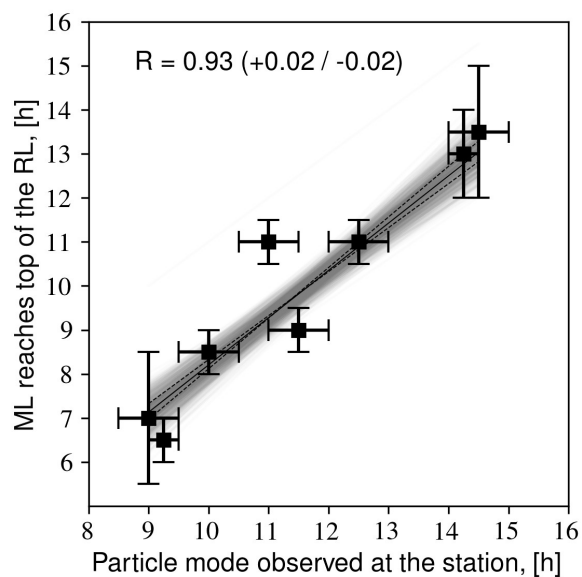
Figure 8: The correlation between the times that a new particle mode coupled with downward particle flux is observed at the field site and the times that the ML reaches the top of the RL.
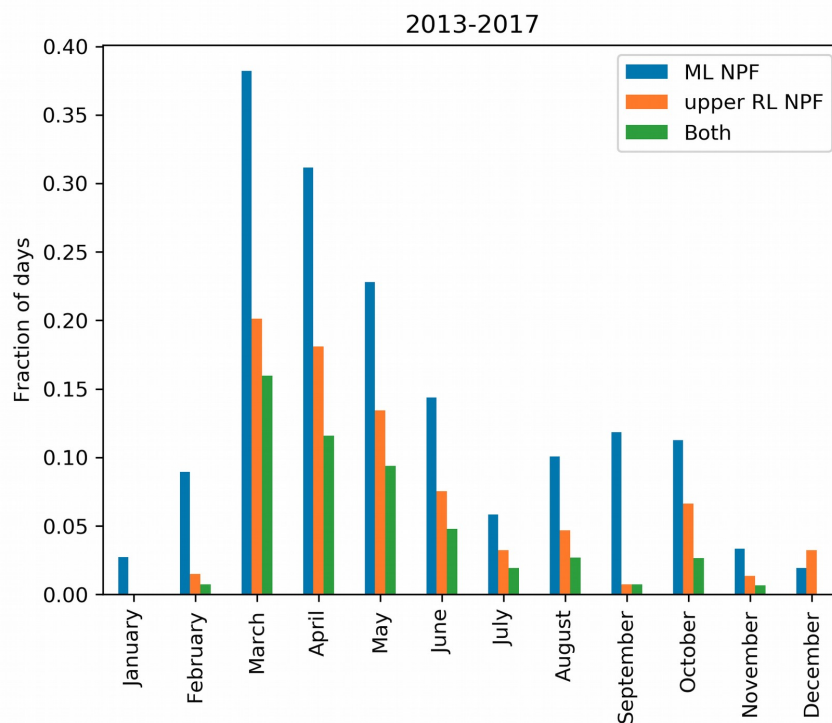
Figure 9: Monthly fractions of NPF within the ML and NPF in the upper RL in Hyytiälä between 2013-2017.
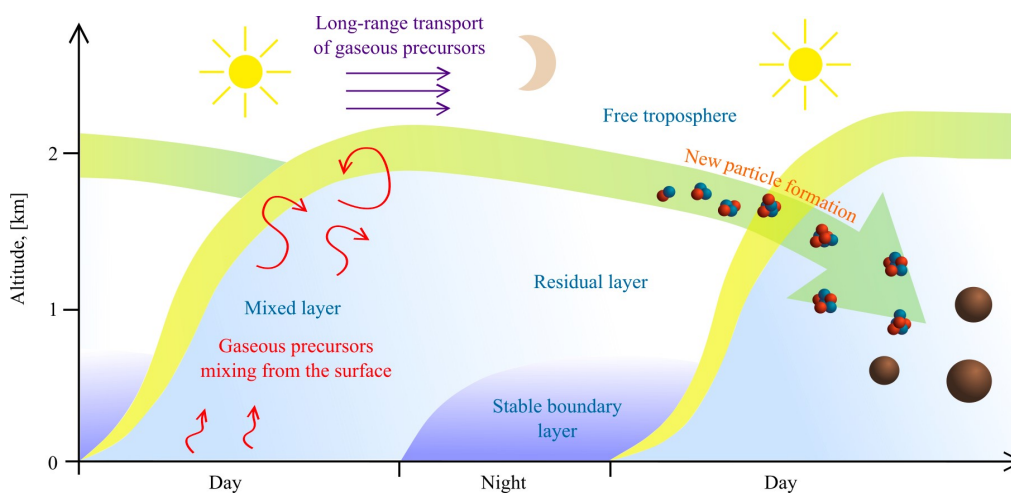
Figure 10: Schematic drawing illustrating the proposed mechanism behind NPF in the upper RL.
Gaseous precursors released from the surface are mixed throughout the ML. When the mixing stops
during the night the gases are stuck in the RL. Also gaseous precursors may be transported in the
FT. In the following morning photochemistry and the thermodynamically favorable conditions in
the upper RL initiate NPF. The freshly formed particles remain in the elevated layer or get mixed
into the a new ML if it reaches the height of the upper RL. The aerosol particles continue to grow
larger, contributing to the aerosol load in the BL.